Article

Not peer-reviewed version

Understanding the Impact of Climate and Seismic Hazard Conditions on Multi-criteria Based Retrofitting of Existing Buildings

Rita Couto , Gianrocco Mucedero , Rita Bento * , Ricardo Monteiro

Posted Date: 11 April 2024

doi: 10.20944/preprints202404.0748.v1

Keywords: seismic retrofit; energy retrofit; MCDM

 doi:10.20944/preprints202404.0748.v1

Article

Understanding the Impact of Climate and Seismic Hazard Conditions on Multi-Criteria Based Retrofitting of Existing Buildings

Rita Couto [1], Gianrocco Mucedero [2,3], Rita Bento [4,*] and Ricardo Monteiro [3,5,6]

[1] PhD Student, University School for Advanced Studies IUSS, Palazzo del Broletto, Piazza della Vittoria n.15, 27100 Pavia, Italy; rita.couto@iusspavia.it
[2] Postdoctoral Researcher—University School for Advanced Studies IUSS, Palazzo del Broletto, Piazza della Vittoria n.15, 27100 Pavia, Italy; gianrocco.mucedero@iusspavia.it
[3] RESISK s.r.l.—Research Engineering for Sustainable Risk Solutions, Pavia, Italy
[4] Full Professor—CERIS, Instituto Superior Técnico, Universidade de Lisboa, Lisbon, Portugal
[5] Associate Professor—University School for Advanced Studies IUSS, Palazzo del Broletto, Piazza della Vittoria n.15, 27100 Pavia, Italy; ricardo.monteiro@iusspavia.it
[6] CONSTRUCT, Faculty of Engineering, University of Porto, Portugal; rncm@fe.up.pt
* Correspondence: rita.bento@tecnico.ulisboa.pt

Abstract: A large share of the reinforced-concrete (RC) building stock in Mediterranean countries faces a dual challenge of seismic vulnerability and energy inefficiency, calling for urgent renovation efforts. While energy upgrades have been the focus of previous renovation policies, recent research highlights the critical need for integrated retrofitting solutions that address both structural integrity and energy performance. Multi-criteria decision making (MCDM) approaches are a promising tool for optimizing the combined choice of these integrated interventions, considering various decision variables (DVs), of economic, social, environmental, and technical nature. To understand the impact of climate and seismic hazard conditions on multi-criteria based retrofitting assessment, a case-study RC school building is selected and assumed to be located in three distinct climate conditions - cold, mild, and warm - and three seismic hazard levels – low, medium and high. Moreover, given the complexity and challenges of quantifying seismic performance metrics for practitioners, an available simplified (practice-oriented) approach is compared herein with a more thorough research-based one for quantifying the seismic performance of RC buildings within the MCDM framework. Both approaches are applied to the case-study building, considering twelve possible combinations of energy and seismic interventions. The accuracy of the practice-oriented approach and its impact on the retrofitting rankings is evaluated, emphasizing the importance of accessible and efficient evaluation methods in facilitating informed decision-making for building renovation.

Keywords: seismic retrofit; energy retrofit; MCDM

1. Introduction

Most of the reinforced-concrete (RC) buildings of the Mediterranean countries stock presents a dual challenge in terms of seismic vulnerability and energy inefficiency, underlying an urgent need for renovation. These buildings have been constructed following outdated guidelines without modern seismic design considerations rendering them susceptible to earthquake damage. Simultaneously, their energy performance is typically highly unsatisfactory. In fact, 75% of the European building stock is energy inefficient, being responsible for 40% and 36% of EU energy consumption and total CO_2 emissions, respectively [1]. Even though Italy is on track to reach the emissions reductions and energy efficiency targets set by its National Energy and Climate Plan (NECP) for 2030 [2], substantial additional efforts need to be made to reach the much more ambitious new targets for 2030 stemming from the European Union's (EU) Fit-for-55 (FF55) package, which

 doi:10.20944/preprints202404.0748.v1

aims to reduce its net greenhouse gas emissions of at least 55% by 2030. Consequently, the renovation of the building sector, in terms of reducing its seismic vulnerability and increasing its energy efficiency, is highly necessary to promote well-being and economic growth and to ensure that the EU energy and climate targets are met [3,4]. for what concerns the Italian context, more than 55% of the RC residential buildings were constructed without seismic provisions and 88% of the Italian masonry and RC buildings do not comply with modern energy performance requirements [5]. According to Gkatzogias and Tsionis (2022) [4], when combining different indicators (seismic, energy, and socio-economic vulnerability), Italy is considered a high priority country for building renovation.

Until recently, renovation efforts and policies were mainly directed to the energy upgrading of buildings alone, without considering their structural performance, because of the immediately evident benefits from the reduced energy costs for heating/cooling. However, if the structural integrity of the retrofitted building is not guaranteed, that same investment could be completely lost, in case of seismic events. Similarly, seismic retrofitting interventions alone could compromise thermal comfort if a building's energy efficiency is not considered. The growing need for renovation of a significant portion of EU buildings has prompted recent advancements in scientific and technical fields, which suggest that adopting an integrated approach to building renovation could lead to improved cost-effectiveness [6]. From a more global perspective, the performance upgrading process is highly influenced by the seismic hazard and vulnerability, energy performance and socio-economic characteristics of the region where the buildings are located, as recently highlighted by Mucedero and Monteiro [7]. Such a study established a regional prioritization framework for seismic and energy efficiency performance upgrading of residential buildings in Italy, revealing that critical regions for seismic retrofitting are primarily in central-southern Italy, while those for energy upgrading are mainly in northern Italy. Although contemporary understanding recognizes that seismic retrofitting cannot be decoupled from energy renovation, the previous two scenarios highlight the need to address this combined retrofitting in a holistic way, to achieve optimal results.

To address both seismic and energy performance concerns, recent research studies have aimed to minimize economic losses and environmental impacts while promoting building renovation. Most of these studies make use of optimization methodologies to identify the ideal solution when a range of several options is available. Multi-criteria decision-making (MCDM) approaches have demonstrated advantages in optimizing combined interventions [8–12]. The MCDM approach for selecting the optimal coupled retrofit intervention can become extremely helpful to decision-makers and practitioners because it encompasses multiple criteria when making decisions about retrofitting options. By considering different decision variables (DVs) chosen to capture the essential aspects of the decision problem (e.g., economic costs, social benefits and technical feasibility), decision-makers can make more informed and balanced decisions.

This study evaluates the influence of climate and hazard levels on the preferential ranking of the retrofit alternatives. To do so, a RC school building is selected as a case study, given the high seismic vulnerability of school buildings in Italy demonstrated by past earthquakes [13], and twelve possible combinations of energy and seismic interventions are identified. Subsequently, the building is assumed to be located in nine different sites characterized by varying levels of seismic hazard and climate conditions. Following an energy and seismic performance assessment, the optimal combined retrofitting intervention is evaluated following a previously-validated MCDM framework [11], for each location considered, resulting in nine distinct rankings.

The detailed analysis methods used to evaluate the seismic performance of different retrofitting alternatives are very computationally expensive and time-consuming, thus, unfeasible to be implemented by practitioners or general decision-makers. With such limitations in mind, this study also evaluates the implementation of a simplified approach to quantify some of the DVs required to select optimal retrofitting strategies for existing buildings. Specifically, the DVs annual probability of failure (APF) and expected annual losses (EAL) are estimated using the cloud-based capacity spectrum method (CB-CSM) and the Italian seismic risk classification procedure (Sismabonus), respectively. The goodness of the simplified approach is further gauged by comparing the MCDM

 doi:10.20944/preprints202404.0748.v1

rankings of combined retrofitting alternatives obtained from using both simplified and refined approaches.

2. Methodology

The MCDM framework, as employed by Clemett et al. (2023) [11] and in subsequent studies [14–16], is adopted herein to identify the optimal combination of seismic and energy retrofitting solutions for a building, when several combination options are feasible. The overall methodology, concluded with the MCDM step, corresponds to a structured process for assessing, designing, and selecting retrofit solutions for buildings exhibiting both seismic and energy deficiencies. This methodology comprises five main steps: assessment, design, performance, decision and selection, which are illustrated in Figure 1

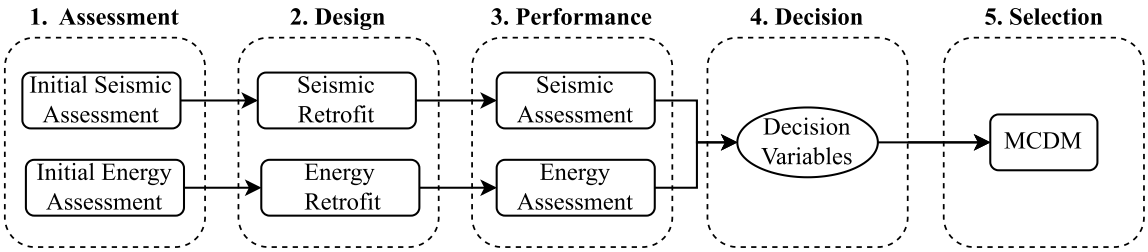

Figure 1. Steps included in the proposed methodology.

Initially, an assessment is conducted to identify the building deficiencies using research-based tools for the seismic performance assessment and commercial energy simulation tools for energy assessment. Thereafter, the design phase involves proposing seismic and energy retrofit solutions based on the identified issues. A performance evaluation is then carried out, using the same tools used in the assessment phase, to quantify the effectiveness of each retrofitting option. The decision-making stage considers various DVs including seismic and energy performance, environmental and social aspects (e.g., architectural impact and duration of works), and technical aspects (such as specialized labour or foundation interventions). The DVs chosen to assess the performance of the retrofitted building are provided in Table 1. Finally, the MCDM process [11] is employed in the selection phase to choose the optimal retrofit alternative and to rank all the selected alternatives. Weight factors are associated with each DV, and their values are highly influenced by the preference of the decision-maker. They are used to quantify the importance of each criterion in the decision-making process, playing a crucial role in determining the relative importance or priority of different criteria or decision variables within the MCDM framework. As a result, weight factors exert a substantial influence on the ranking of the alternatives [17]. The weight factors selected in this study are based on the work of Clemett et al. [17] and shown in Table 1: more emphasis is placed on the installation cost and duration of works of the retrofit intervention, as well as the seismic performance (in terms of APF and EAL) and the energy performance of the building.

Table 1. Decision variables considered for the MCDM framework.

Group	Decision Variables		Weight
Economic	C_1	Installation cost	0.15
	C_2	Expected annual costs (EAC)	0.19
Environmental	C_3	Expected life-cycle environmental impacts (LCEI)	0.18
Social	C_4	Annual probability of failure (APF)	0.14
	C_5	Duration of works	0.13
	C_6	Architectural impact	0.06
Technical	C_7	Need for specialized labour/design knowledge	0.05
	C_8	Required intervention at the foundations	0.10

 doi:10.20944/preprints202404.0748.v1

In this approach, the highest computational burden is mostly associated with the quantification of some of the DVs (obtained from the results of steps 1 and 3 in Figure 1), if refined, research-based tools are used. Such DVs are the annual probability of failure (APF), considered – C_4 – the expected annual losses (EAL) and expected annual environmental impact (EAEI) – C_2 and C_3, respectively. Detailed seismic assessment is usually conducted using incremental dynamic analysis (IDA) or multiple-stripe analysis (MSA) to obtain the fragility parameters and, subsequently, the APF. In turn, within a lower-refinement level of analysis, more likely to be used in the engineering practice field, nonlinear static analysis-based procedures, such as the SPO2IDA tool [18], the SPO2FRAG tool [19] or the incremental N2 method [20] can be considered to perform collapse fragility estimation. On the other hand, comprehensive performance-based loss estimation (component-based approach - PEER-PBEE methodology [21]) or simplified tools (e.g., Storey Loss Functions [22,23], the DEAL approach [24]) are usually implemented to obtain the expected annual loss (EAL) and the expected annual environmental impact (EAEI).

This study adopts a simplified approach to estimate the aforementioned computationally onerous DVs. In particular, the APF is quantified through the results of the cloud-based capacity spectrum method (CB-CSM) [25], while, for the loss assessment, the simplified procedure outlined in the Italian guidelines for seismic risk classification of constructions (Sismabonus) [26] is chosen, replacing the cumbersome component-based approach implemented in the PACT software [27]. In the following sections, a brief description of the detailed and simplified approaches employed in this study is provided.

2.1. Detailed Approach

The detailed approach for the estimation of the DVs C_2, C_3 and C_4 follows a comprehensive performance-based seismic assessment and loss analysis through the PEER-PBEE methodology. The procedure initiates with the characterisation of the seismic hazard at the selected site, followed by a selection of suitable hazard-consistent ground motion sets. Then, nonlinear time history analysis is conducted on the structure under analysis, using the previous set of selected ground motions, through multiple-stripe analysis (MSA), which allows the quantification of the structural response. Through the MSA results, collapse fragility parameters are derived. Expected damage and loss are quantified considering structural and non-structural components thus it is necessary to develop an inventory of damageable components in the building, together with the definition of their potential damage states, expected repair cost and environmental impact consequences. Finally, the detailed seismic loss assessment is performed through PACT [21]. The ultimate outcomes needed for the MCDM framework are the EAL, the EAEI and the APF.

2.2. Simplified Approach

The simplified counterpart makes use of two readily-available tools to estimate the AFP and EAL, namely the Cloud-based Capacity Spectrum Method (CB-CSM) and Sismabonus, respectively. The CB-CSM is a combination of two well-established methods, the capacity spectrum method (CSM) [28] and the cloud-based (CB) procedure [29], to estimate the collapse fragility parameters of a given structure. The method starts with the identification of the performance point (PP) of the structure with the CSM. Since multiple PPs can be obtained, several recommendations on how to overcome this problem and select the most suitable PP are available in [25]. In this study, in case of multiple PPs, the adopted PP was the one for which the absolute difference between the geometric average of spectral displacements over an appropriate range of periods (AvgSdk) and each obtained PP ($|AvgSdk - \Delta PP|$) is minimum. This procedure leads to a cloud of Engineering Demand Parameter (EDP) vs Intensity Measure (IM) points for each analysed Single Degree of Freedom (SDoF) system. The EDP is the target displacement corresponding to the PP calculated via CSM and the adopted IM is the geometric mean of the spectral accelerations (AvgSa) computed in the interval $[0.2T_{el} - 1.5T_{el}]$, with T_{el} being the elastic period of the structural system, as recommended in [25]. Based on the criteria selected to define the collapse limit state, the cloud data is divided into non-collapse (NoC) and

 doi:10.20944/preprints202404.0748.v1

collapse (C) points and the collapse fragility parameters are calculated through the total probability theorem.

Sismabonus is a relatively recent procedure implemented in Italy to evaluate the seismic risk of buildings and use it to classify them [26]. This guideline provides a simple method for practitioners to assess the building's initial seismic condition and estimate its expected yearly seismic losses. This estimation can also help in evaluating the effectiveness of different retrofitting strategies in improving the building's seismic performance hence to guide the choice of the retrofitting strategy. Notably, the Sismabonus approach requires only nonlinear static analysis, making it a more practical and quicker method to evaluate seismic annual losses, when compared to approaches like the PEER-PBEE [21]. Furthermore, when compared to other available simplified procedures for estimating the EAL of a building, Sismabonus holds additional advantages as it is already in use within the Italian engineering practice, even if recent findings show its loss estimates to be more conservative, when compared to the ones obtained with more refined methodologies [30,31]. This method requires the computation of two performance indices: the Building Safety Index (SI-LS) and Expected Economic Annual Losses (EAL). The SI-LS is calculated determining the capacity peak ground acceleration (PGAC) and demand peak ground acceleration (PGA_D) associated with the Life Safety Limit State (LSLS). Concurrently, the EAL is estimated by considering the building's performance for various return periods (T_r) and repair costs expressed as a fraction of the Reconstruction Cost (%RC). The resulting loss curve, which defines the seismic risk, is represented by a point ($1/T_r$, %RC) for each limit state, whereas the area underneath is the EAL. The overall risk class of the building is defined as the worst between SI-LS and EAL classes. This method integrates structural and economic considerations, providing a comprehensive framework for seismic risk assessment. More details on the procedure can be found in the work by Cosenza et al. [26].

3. Application to a Case-Study Building

The selected case-study school building is a reinforced concrete (RC) moment resisting frame (MRF) with unreinforced masonry (URM) infills, located in Isola del Gran Sasso d'Italia (Abruzzo, Italy) and built between the 1960s and 1970s (Prota et al., 2020). The building has two aboveground storeys with roughly 630 m^2 each and inter-story heights of 3.75 and 4.25 m, on the first and second floors. Additionally, there is a small partial basement at the east end. The structural system consists of two-way RC MRFs in the longitudinal and transverse directions, along with URM infills and partitions. More details on the school building, including architectural plans and elevations, together with the material properties of structural members, can be found in Prota et al. [32]. The masonry infills were assumed to have the same geometry and material properties as the medium-strong masonry infill typology in the macro-level classification as proposed in [33]. The numerical model of the building, comprising flexural elements (for beams and columns), beam-column joints (BCJs), a staircase, and masonry infills, was developed in OpenSees [34], and a three-dimensional representation of the model is presented in Figure 2. Further details on the numerical modelling of the structure can be found in [11,35].

Preprints.org (www.preprints.org) | NOT PEER-REVIEWED | Posted: 11 April 2024 doi:10.20944/preprints202404.0748.v1

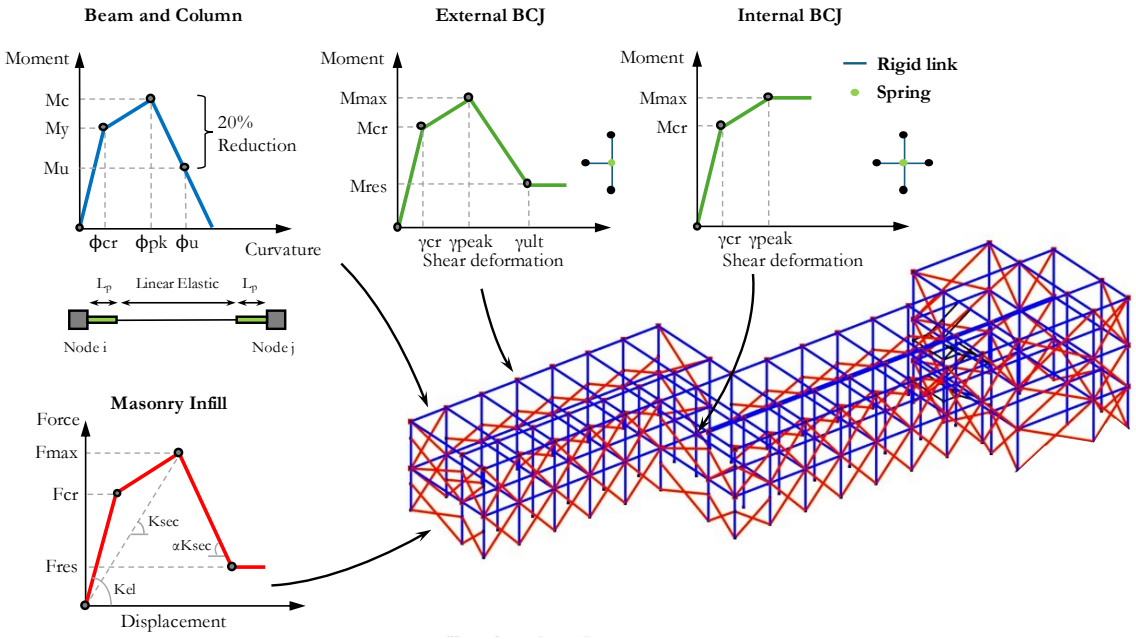

Figure 2. Numerical model of the case-study building, developed in OpenSees [11].

For the purposes of this study, i.e. understanding the influence of seismic hazard level and climate conditions on the combined retrofitting, the building is assumed to be located in nine different sites in Italy: three sets of different hazard levels, namely high (H), medium (M) and low (L), paired with three sites characterized by different climatic conditions, namely cold (C), moderate (M) and warm (W). Choosing real locations in Italy was intended to ensure the results of this study closely reflect actual conditions. However, this decision may introduce uncertainty when assessing and comparing the results due to variations in seismic hazard curves and the corresponding selection of records.

The specific features of each site are summarized in Table 1 with the indication of the peak ground acceleration (PGA) for the life safety limit state (SLV), defined according to the Italian code (NTC-2018) [36] and the heating degree days (HDD) for each location. The latter is a measure used to estimate the heating energy demand, calculated by summing the number of degrees that the outdoor temperature falls below a certain base temperature on each day over a specified period. It is used to estimate heating energy requirements such as consumption patterns, performance, and costs. Figure 3 provides the acceleration response spectrum and the hazard curve for each selected site. Even though the PGA of each location within the same seismic hazard level group is very similar, as anticipated, the corresponding hazard curves show some differences.

Table 2. Main features of selected case-study sites.

City	ID	Coordinates	Level of seismicity	PGA (SLV) [g]	Climatic zone	Heating Degree Days (HDD)
Città di Castello	H-C	43.4700°N, 12.2314° E	High (H)	0.30	Cold (C)	2347
Isola del Gran Sasso d'Italia	H-M	42.5056°N, 13.6592° E		0.29	Moderate (M)	2038
Catania	H-W	37.5013°N, 15.0742° E		0.29	Warm (W)	833
Vicenza	M-C	45.5455º N, 11.5354º E	Medium (M)	0.21	Cold (C)	2371
Serravalle Pistoiese	M-M	43.9059º N, 10.8330º E,		0.20	Moderate (M)	2010

Preprints.org (www.preprints.org) | NOT PEER-REVIEWED | Posted: 11 April 2024 doi:10.20944/preprints202404.0748.v1

Cirò Marina	M-W	39.368º N, 17.128º E	Low (L)	0.21	Warm (W)	845
Alessandria	L-C	44.9073° N, 8.6117° E		0.08	Cold (C)	2559
Genova	L-M	44.4056° N, 8.9463° E		0.10	Moderate (M)	1435
Agrigento	L-W	37.3089° N, 13.5858° E		0.08	Warm (W)	729

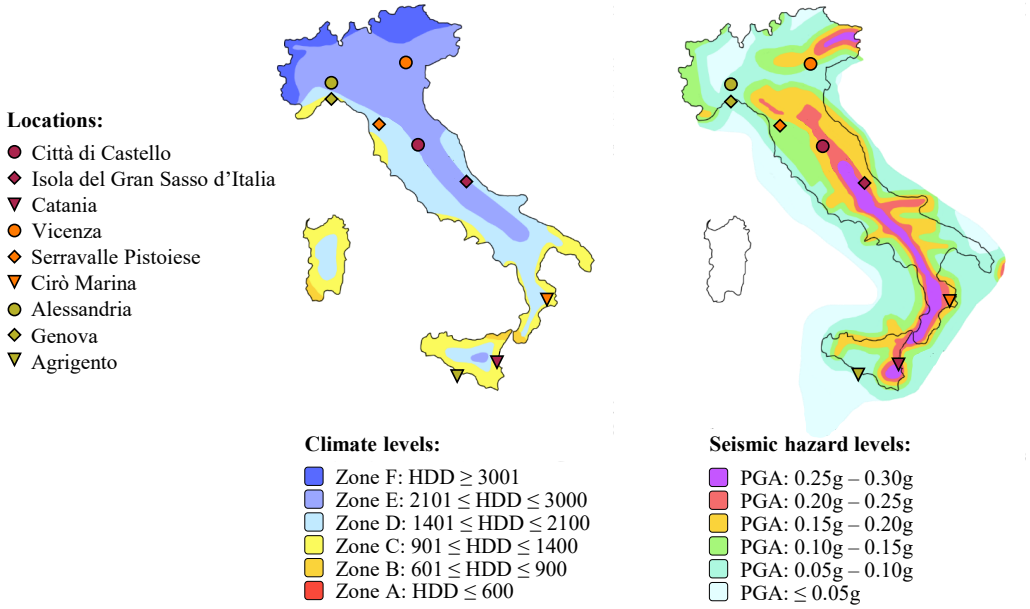

Figure 3. Climate and seismic hazard levels maps of Italy, with the indication of the selected locations under study.

3.1. Prelimianry Seismic Assessment

A preliminary seismic assessment of the structure was conducted following a nonlinear static procedure as established in the Italian seismic code [36]. The target displacements of the structure for the collapse limit state (SLC) using the N2 method [37] were estimated and compared with the performance point displacements at which the structure attains its capacity for the SLC limit state, considered to be reached as soon as one of the following performance criteria is met:

- The shear force demand exceeds the shear capacity of one or more of the beam or column elements;
- The chord rotation of one or more of the plastic hinges in the beam, column, or wall elements exceeds the collapse limit state deformation limits;
- The shear deformation in one or more of the beam-column joints (BCJs) exceeds 0.02 rad.

The first two performance criteria are the ones prescribed by the Italian seismic code [36] for the seismic assessment of columns and beams. The last criterion, regarding the assessment of the BCJs, was adopted following experimental evidence [38], given that the one foreseen by the Italian code is very conservative. The pushover curves of the as-built structures, together with the performance points (SLC_C) and target displacements (SLC_D) of the structure for each site are presented in Figure 4.

Preprints.org (www.preprints.org) | NOT PEER-REVIEWED | Posted: 11 April 2024 doi:10.20944/preprints202404.0748.v1

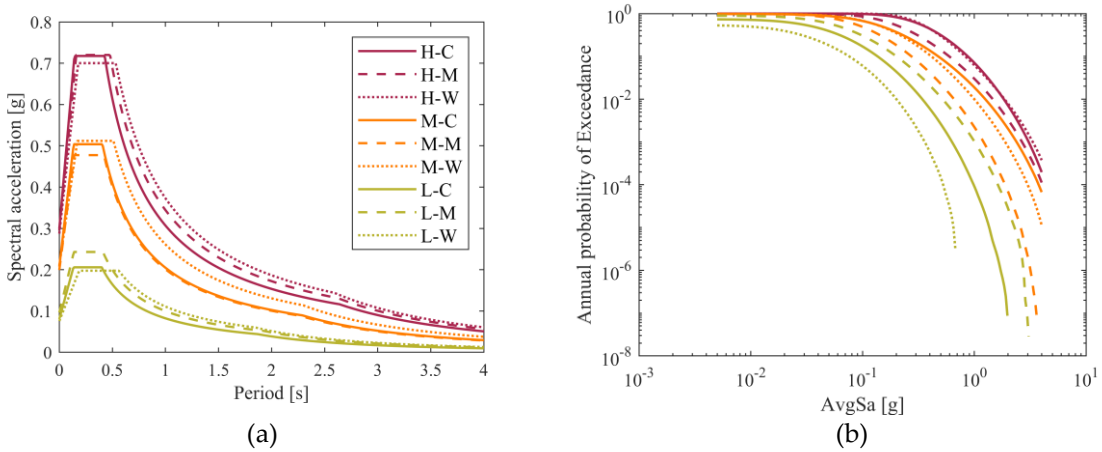

Figure 4. (a) Acceleration response spectra and (b) hazard curves for the six analysed sites.

Both directions present pushover curves with similar initial stiffness but different degradation, due to the larger number of openings on the masonry infills in the longitudinal direction of the building. For both directions, the main structural weaknesses at the collapse limit state were identified as the shear failure of columns that were not designed to withstand seismic actions. Given the different demand of each set of sites, different target displacements are obtained; for the LH sites, the safety performance of the structure in its as-built condition is achieved in the X direction and almost achieved in the Y direction.

Following the Italian "Guidelines for the seismic risk classification of the constructions" [39], the safety index of the structure (SI-LS), defined as the ratio between the capacity peak ground acceleration (PGA_C) and the demand peak ground acceleration (PGA_D), was calculated and is summarized in Table 3. PGA_C was assumed to be the one that caused the collapse of the building, according to the previously described criteria. PGA_D is defined as the PGA of the code-based response spectrum that intersects the pushover curve on its capacity point.

The obtained SI-LS values reveal, as anticipated, variations in demand across the different sites, with direction Y emerging as the most critical. Considering the satisfactory performance of the as-built structure for the low hazard sites, retrofitting was deemed unnecessary hence different retrofitting schemes were solely considered for sites with moderate and high hazard levels, as addressed in the next sections.

Table 3. Seismic safety index (SI-LS), in percentage, of the as-built structure, as a function of the level of hazard and climate conditions (critical direction in bold).

Direction	Low hazard			Medium hazard			High Hazard		
	L-C	L-M	L-W	M-C	M-M	M-W	H-C	H-M	H-W
X	135	115	140	55	58	54	39	40	39
Y	**95**	**81**	**98**	**38**	**41**	**38**	**27**	**28**	**27**

3.2. Seismic Retrofit Interventions

Given the structural deficiencies identified in the preliminary seismic assessment of the building, four different seismic retrofit measures (SRMs) were considered:

- S_1: local strengthening with carbon FRP (CFRP);
- S_2: global strengthening with concentric steel braces;
- S_3: CFRP strengthening combined with concentric steel braces;
- S_4: CFRP strengthening combined with viscous dampers.

Additionally, for all SRMs, a seismic gap between the URM infills and the RC frame was introduced, reducing the column-infill interaction and, thus, the shear forces acting on the columns. The design of the SRMs, conducted following the Italian building code (NTC) [36], was carried out

 doi:10.20944/preprints202404.0748.v1

to address the weaknesses and improve the performance of the as-built structure as much as possible, with the acknowledgment that the achieved performance was not always that required for new code-conforming buildings due to practical and cost considerations [40]. Considering the varying seismic hazard levels across each site, the extent of retrofitting interventions implemented for the case-study building was adjusted accordingly. Due to the poor performance of the building under high seismic hazard conditions, each intervention was designed to provide the optimal contribution to the structure meaning that it was not strictly designed for the same seismic demand. Consequently, it did not strictly achieve the same threshold in terms of capacity between the several alternatives. Table 4 provides a summary of the details and quantities of the retrofit components for each retrofit alternative.

Table 4. Retrofit components and corresponding amount per alternative for the considered hazard levels.

Retrofit Alternative		Units	Medium hazard	High hazard
S_1	Column wrap	m^2	245.1	352.6
	Column bar	m	2972	2972
	Beam wrap	m^2	177.8	256.2
	Joint wrap	m^2	138.2	186
S_2	Braced bays	Nr	9	10
S_3	Column wrap	m^2	5.1	10.2
	Column bar	m	272.0	272.0
	Beam wrap	m^2	11.7	31.22
	Joint wrap	m^2	45.5	45.5
	Braced bays	Nr	10	10
S_4	Column wrap	m^2	-	10.2
	Column bar	m	-	456
	Beam wrap	m^2	-	33.7
	Joint wrap	m^2	53.4	53.4
	Viscous dampers	Nr	36	36

3.3. Energy Retrofit Interventions

Subsequently, with a view to improve the energy performance, three different energy retrofit measures (ERMs) were considered:

- E_1: roof insulation, installation of efficient LEDs and thermostatic valves on radiators;
- E_2: intervention E_1 coupled with external wall insulation with expanded polystyrene (EPS) panels;
- E_3: intervention E_2 coupled with installation of efficient windows, floor insulation, condensing boiler, lighting control system, and photovoltaic panels.

Each energy retrofitting intervention aims to simultaneously reduce heat losses to the external environment and enhance the energy efficiency of systems within the building. The level of intervention increases from E_1 to E_3, according to the Italian Ministerial Decree [41], which also corresponds to a higher degree of invasiveness.

Finally, the four seismic interventions were coupled with each energy intervention, leading to twelve possible combined retrofit alternatives. Each coupled intervention is designated by S_iE_i, where S_i and E_i correspond, respectively, to the considered seismic and energy retrofit schemes. More information on the design procedures and assumptions can be found in previous studies [11,42,43]. Table 5 summarizes the intervention cost, in €/m^2, and the duration of work, in days, corresponding to DVs C_1 and C_5, respectively. The intervention cost corresponds to the combined cost of the seismic and energy retrofit schemes for each alternative, considering efficiencies that can be gained simultaneously by implementing both retrofitting schemes. The total cost of installation of each retrofit alternative includes, in addition to the cost of the retrofit material, the removal of internal

 doi:10.20944/preprints202404.0748.v1

linings, partial demolition of the existing structure/infills, removal of debris, installation of the retrofit scheme, and restoration of infills and lining. More details on the energy retrofit costs can be found in [11].

Table 5. Intervention cost (C_1) and duration of works (C_5) for each retrofit alternative per level of hazard.

Alt	Medium Hazard						High Hazard					
	Cold		Moderate		Warm		Cold		Moderate		Warm	
	C_1 (€/m²)	C_5 (days)	C_1 (€/m²)	C_5 (days)	C_1 (€/m²)	C_5 (days)	C_1 (€/m²)	C_5 (days)	C_1 (€/m²)	C_5 (days)	C_1 (€/m²)	C_5 (days)
S_1E_1	529	38	525	38	507	38	867	60	881	61	871	63
S_1E_2	589	38	568	38	543	38	927	60	925	61	908	63
S_1E_3	753	42	692	42	671	42	1091	64	1048	65	1036	67
S_2E_1	135	21	131	21	113	21	136	22	132	22	114	22
S_2E_2	196	23	175	23	150	23	196	24	175	24	150	24
S_2E_3	359	28	298	28	277	28	360	29	299	29	278	29
S_3E_1	172	23	168	23	150	23	180	37	213	42	195	42
S_3E_2	232	23	211	23	186	23	240	37	257	42	232	42
S_3E_3	396	27	335	27	314	27	404	41	380	46	360	46
S_4E_1	289	14	284	14	266	14	437	44	419	44	381	43
S_4E_2	349	27	328	27	303	27	499	44	463	44	418	43
S_4E_3	513	31	451	31	431	31	661	48	586	48	546	47

3.4. Post-Intervention Seismic Assessment

The post-intervention assessment followed the same strategy outlined for the as-built structure (S_0). Nonlinear static analyses were performed for each retrofitted model, and the displacement demand and capacity (according to NTC [36]) were computed using the N2 method [37]. The results for the retrofitting scenarios are illustrated in Figure 5.

Preprints.org (www.preprints.org) | NOT PEER-REVIEWED | Posted: 11 April 2024 doi:10.20944/preprints202404.0748.v1

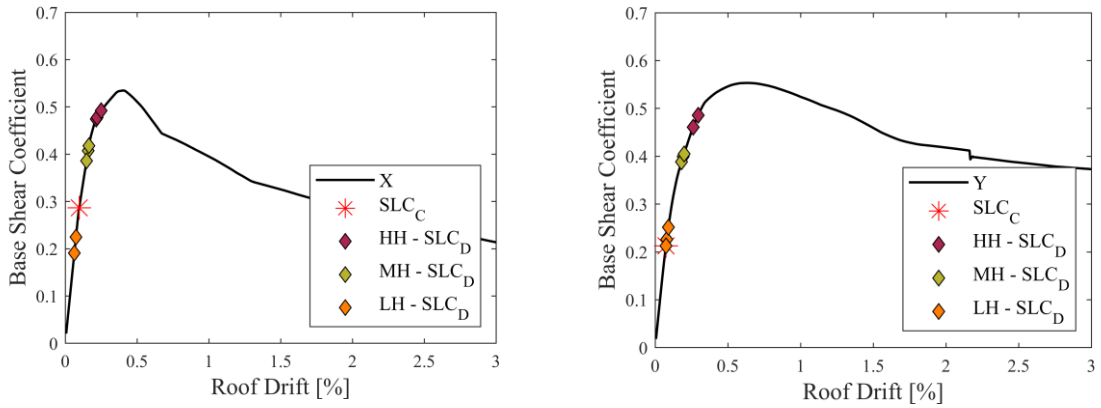

Figure 5. Preliminary seismic assessment of the as-built structure pushover curves in the X (left) and Y (right) direction, with the indication of the N2 performance points for the SLC limit state and the target displacement as a function of the hazard level.

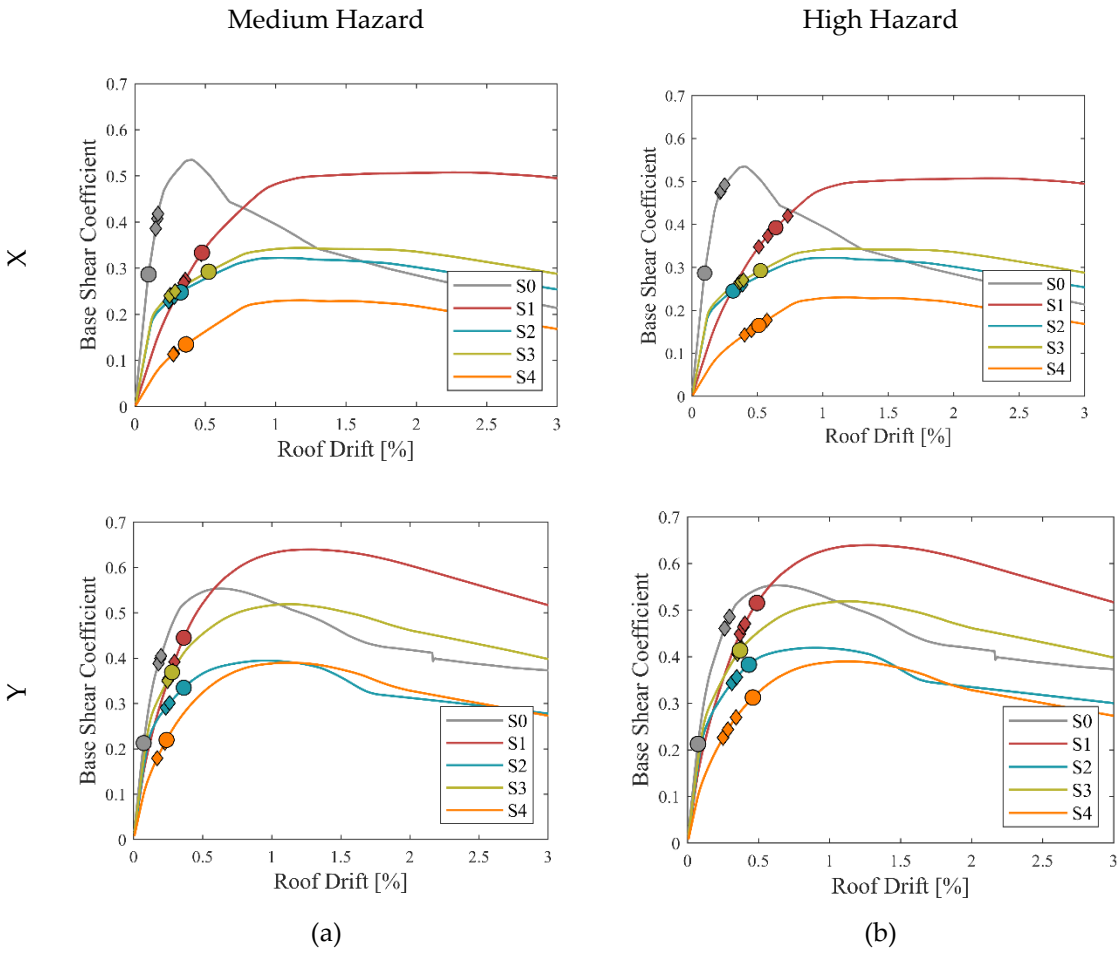

Figure 6. Post-seismic intervention assessment of the structural retrofit schemes: pushover curves in the X and Y direction, with capacity (circles) and N2 performance points (diamonds) for the SLC limit state, as a function of the hazard level: (a) medium and (b) high hazard.

At a first glance, it can be observed that the pushover curves for the same type of retrofit intervention between the different levels of hazard are very similar. This can be justified by the similarity of each retrofit intervention between the different sites, both in terms of their layout within the building structure and specific structural elements being retrofitted. When compared with the as-built scenario, all retrofitted models exhibit a decrease in the initial stiffness and lateral strength due to the seismic gap introduced between the infills and the surrounding frame. Moreover, all the retrofit

 doi:10.20944/preprints202404.0748.v1

interventions lead to an improvement in the structural performance of the building at the collapse limit state. Given the different design levels of the retrofitting interventions (dictated by the different seismic hazard levels), the displacement for which the structure, with the same type of intervention, reaches its capacity is distinct. Nevertheless, for most of the cases, the type of structural failure - usually a brittle failure on a column or beam as mentioned previously - that dictates the capacity performance is similar.

Table 6 summarizes the SI-LS values obtained for the retrofitted models in each hazard site. Considering the most critical direction, the effectiveness ranking of the retrofit measures is $S_4 > S_1 > S_3 > S_2$ and $S_1 > S_4 > S_3 > S_2$ for the medium and high hazard site at the LSLS. Comparing the results of Table 3 with Table 6 an overall improvement is observed on the performance of the retrofitted structures with respect to the as-built structure.

Table 6. Seismic safety index (SI-LS) of each structural intervention, S_i, for the different levels of hazard and climate conditions (critical direction in bold).

Alt.	Dir.	Medium hazard			High Hazard		
		M-C	M-M	M-W	H-C	H-M	H-W
S_1	X	**120 %**	**123 %**	**95 %**	**120 %**	**108 %**	**99 %**
	Y	134 %	134 %	105 %	120 %	107 %	109 %
S_2	X	**92 %**	**95 %**	**73 %**	**63 %**	**55 %**	**50 %**
	Y	113 %	115 %	88 %	85 %	76 %	70 %
S_3	X	122 %	125 %	**96 %**	**82 %**	**73 %**	**68 %**
	Y	**111 %**	**113 %**	99 %	87 %	77 %	76 %
S_4	X	**125 %**	**128 %**	**97 %**	**117 %**	**105 %**	**96 %**
	Y	127 %	130 %	99 %	155 %	137 %	129 %

After conducting the initial seismic assessment of the structure in its retrofit conditions, the estimation of all the DVs outlined in Section 2 can be carried out following the suggestions provided in [11]. The ones for which the use of simplified procedures is proposed (C_2, C_3 and C_4) are fully described in the subsequent subsections.

3.4.1. Annual Probability of Failure

The estimation of APF was assessed through different approaches as mentioned in Section 2. To apply the detailed methodology, firstly, the characterization of the seismic hazard at the selected site for the case-study building was carried out through probabilistic seismic hazard analysis (PSHA) using OpenQuake [44]. Then, a selection of 20 pairs of suitable hazard-consistent ground motion records was carried out for each site. The selected IM (AvgSA) is defined as the geometric mean of the pseudo-spectral acceleration in a structure-specific range of periods depending on the first-mode periods of the case studies. Table 7 summarizes some dynamic elastic properties of the analysed models such as the fundamental period in both directions (first mode in bold), the participation mass of the first mode of vibration (M_1^*), the geometric mean (T_{GM}) and the period range used in this study ($0.2T_{GM} - 1.5T_{GM}$). MSAs were conducted and a set of selected EDPs – absolute Peak Floor Acceleration (PFA), Peak Story Drift (PSD), and Peak Floor Velocity (PFV) – were recorded and later used as input to perform the comprehensive performance-based loss assessment (PEER-PBEE methodology). Additionally, the MSA outcomes were also used to determine the collapse fragility parameters.

Following the simplified methodology, a set of 200 ground motions, covering a wide range of magnitudes, were selected from the NGA-West2 ground motion database [45] and converted into the ADRS format to apply the CSM [28] outlined in Section 2.2. The intersection of the capacity curve of the SDoF system of each model with the response spectrum of the selected ground motions results in a cloud of PPs for each retrofitted model. The cloud PPs were filtered into non-collapse (NoC) and collapse (C) data by comparing the obtained PPs with the displacements at which the collapse of the structure is assumed to occur (consistently assumed as those considered for the preliminary assessment and MSA). Lastly, the regression parameters to establish the conditional probability of

Preprints.org (www.preprints.org) | NOT PEER-REVIEWED | Posted: 11 April 2024 doi:10.20944/preprints202404.0748.v1

exceedance were estimated based on the modified cloud analysis procedure outlined in Jalayer et al. (2017) [29]. A slight modification of the CB-CSM procedure was needed to assess the structural performance of S_4, to account for the supplemental damping introduced by the viscous dampers. A supplemental damping ratio of 25%, in addition to the initial 5% damping, was considered in the time history analyses and within the CSM procedure as suggested in [35].

The collapse fragility curves computed through both approaches and accounting for the epistemic uncertainties [46–48] for the medium and high hazard sites are summarized are displayed in Figure 7.

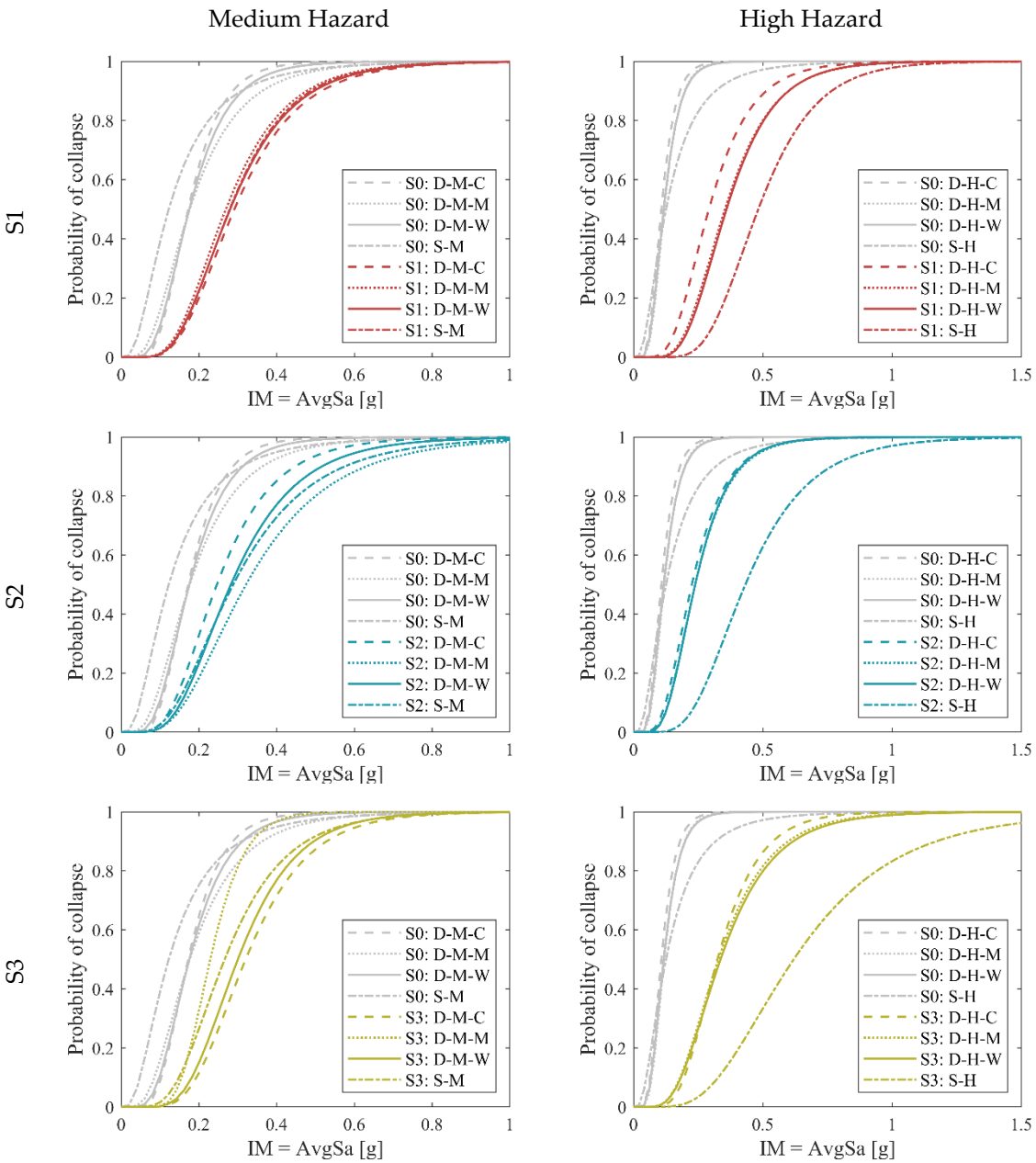

 doi:10.20944/preprints202404.0748.v1

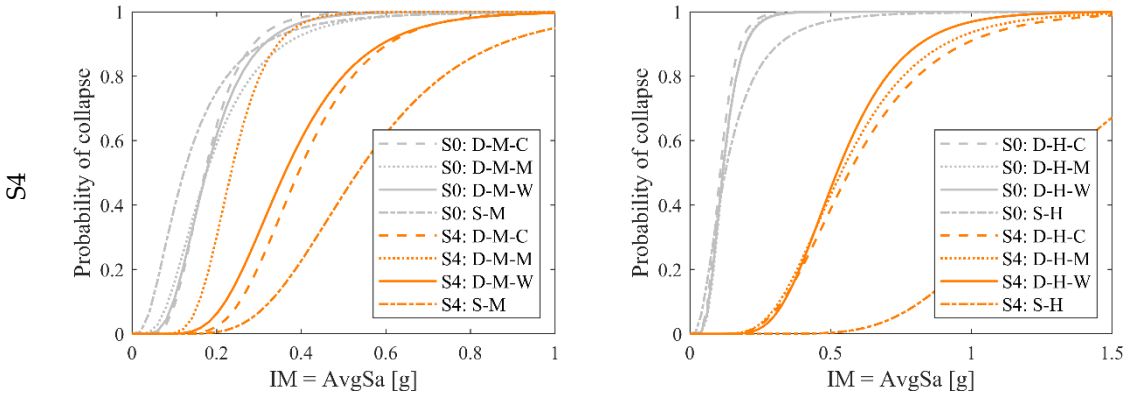

Figure 7. Collapse fragility curves for different hazard levels and retrofitted buildings.

Table 7. Model parameters of each retrofitted building.

Hazard level	Model	Fundamental period [s]		M_1^* [%]	T_{GM}	$0.2T_{GM} - 1.5T_{GM}$
		Longitudinal	Transverse			
Medium hazard	S_0	0.235	**0.267**	38.0	0.25	0.05 - 0.38
	S_1	**0.561**	0.454	39.3	0.50	0.10 - 0.76
	S_2	**0.408**	0.379	47.1	0.39	0.08 - 0.59
	S_3	**0.405**	0.379	46.1	0.39	0.08 - 0.59
	S_4	**0.779**	0.565	41.5	0.66	0.13 – 1.00
High hazard	S_0	0.235	**0.267**	38.0	0.25	0.05 - 0.38
	S_1	**0.571**	0.454	40.4	0.44	0.09 - 0.67
	S_2	**0.407**	0.373	44.0	0.39	0.08 - 0.60
	S_3	**0.405**	0.365	43.9	0.38	0.08 - 0.60
	S_4	**0.785**	0.563	41.4	0.59	0.12 – 0.90

Considering the medium hazard sites, the differences in the median collapse intensities obtained through the detailed approach are likely justified by the different hazard curves observed in Figure 3b. In contrast, the median collapse intensities for the high hazard sites are very similar. Comparing the simplified with the detailed approach, a closer approximation of the median intensity values is achieved for the medium hazard, with a difference of about ±15% (excluding S_0 and S_4). This difference increases up to ±80% when considering the high hazard results. For the S_4 alternative, the simplified approach results in extremely conservative results (an average difference of around 43% and 136% for the medium and high-hazard sites).

Subsequently, the APF values were obtained integrating the collapse fragility curve with the hazard curve of each site. Figure 7 plots the APF values as a function of the employed methodology (simplified (S) and detailed (D)) for both seismic hazard levels – medium (Figure 7a) and high (Figure 7b).

 doi:10.20944/preprints202404.0748.v1

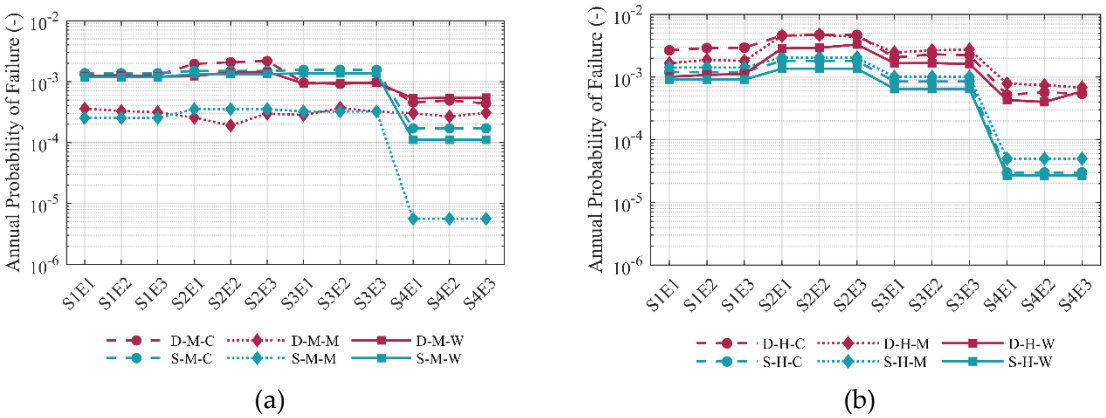

(a) (b)

Figure 8. APF obtained employing the detailed and simplified methodologies for: (a) medium and (b) high hazard sites.

In terms of retrofitting approaches, for medium hazard, solution S_4 has the better seismic performance followed by S_1, S_2 and S_3 with identical performance. For the high hazard, solutions S_2 and S_4 have the worst and better seismic performance, whereas the performance of S_1 and S_3 oscillate between the second and third positions.

For the medium hazard sites, overall, both approaches lead to very similar APF results, except for solution S_4, for which the simplified APF estimates result lower than the detailed ones. On the other hand, for high hazard, regardless of the retrofitting option, the APF results can be considered in two groups, depending on the adopted approach. A general underestimation of the simplified APF values is observed with respect to the detailed ones. Among other possible reasons, it can be related to the fact that the adopted CSM procedure is the one from ATC-40 [28], which has shown to underestimate the displacement demand [49,50], resulting in a lower number of collapses. Still, the differences are never high enough to change the corresponding ranking (when solely based on the APF values) of the different retrofit alternatives.

3.4.2. Expected Annual Losses (EAL) and Expected Annual Environmental Impacts (EAEI)

On the detailed approach side, the PEER-PBEE methodology [51] was employed to estimate the EAL and EAEI of each retrofitted model. By handling the EDP results obtained in the MSA, and by adopting an inventory of damageable components in the building, their potential damage states, and expected repair cost and EI consequences, a detailed loss assessment was carried out in PACT (FEMA P-58). The presence of the ERMs was accounted for at this stage in terms of additional repair consequences to specific non-structural components due to their significant influence on the loss assessment. Regarding the simplified approach, the procedure outlined in Section 2.2 was carried out to obtain the seismic risk classification of each retrofitted structure using Sismabonus [26]. The SI-LS index, defined as the ratio between the capacity peak ground acceleration (PGA_C) and the demand peak ground acceleration (PGA_D), used previously to compare the seismic performance of the retrofitted structures, is summarized in Table 3 and Table 6 for the X and Y directions of the as-built and retrofitted configurations, respectively. The SI-LS index and corresponding risk classification for the critical direction of the as-built and each retrofitted model are summariaed in Table 10. The expected annual environmental impacts (EAEI) are obtained employing the detailed methodology within the loss assessment procedure through PACT. As such, when using the simplified procedure (Sismabonus), which does not enable the direct quantification of the EAEI, the results from the detailed methodology were used to fit a linear regression model between EAL and EAEI. The regression is then used to estimate, in a simplified manner, the EAEI straight from EAL (Couto et al. (2024)).

Preprints.org (www.preprints.org) | NOT PEER-REVIEWED | Posted: 11 April 2024 doi:10.20944/preprints202404.0748.v1

Table 8. Sismabonus results.

Alt.	Param.	Medium hazard									High hazard								
		M-C			M-M			M-W			H-C			H-M			H-W		
		%	Class		%	Class		%	Class		%	Class		%	Class		%	Class	
S_1	SI-LS	120	A^+	A^+	123	A^+	A^+	95	A	A	120	A^+	A	108	A^+	A	99	A	A
	EAL	0.46	A^+		0.48	A^+		0.52	A		0.61	A		0.61	A		0.64	A	
S_2	SI-LS	92	A	A	95	A	A	73	B	B	63	B	B	55	C	C	50	C	C
	EAL	0.49	A^+		0.51	A		0.59	A		0.80	A		0.82	A		0.60	A	
S_3	SI-LS	111	A^+	A^+	113	A^+	A^+	96	A	A	82	A	A	73	B	B	68	B	B
	EAL	0.46	A^+		0.46	A^+		0.50	A		0.63	A		0.67	A		0.65	A	
S_4	SI-LS	125	A^+	A^+	128	A^+	A^+	97	A	A	117	A^+	A	105	A^+	A	96	A	A
	EAL	0.42	A^+		0.43	A^+		0.47	A^+		0.52	A		0.54	A		0.52	A	

The EALs of each retrofitted model, obtained through the detailed and simplified methodologies for both seismic hazard levels, are summarised in Figure 9. For all sites considered, the simplified methodology leads to greater values of EAL, when compared with those of the detailed methodology. This overestimation can be attributed to the simplifications foreseen by the procedure to make it more accessible to engineers, such as the fixed percentage of repair costs for each damage state, regardless of the building typology and their structural response [23,53]. For the high hazard sites (H), S_2 presents the highest EAL, followed by S_3, S_1, and, finally, S_4, regardless of the approach employed, and site considered. For the medium hazard sites, the EAL values from the detailed approach exhibit the same order of magnitude (S_2>S_3>S_1>S_4) while the results obtained with the simplified approach exhibit different orders of magnitude as a function of the site.

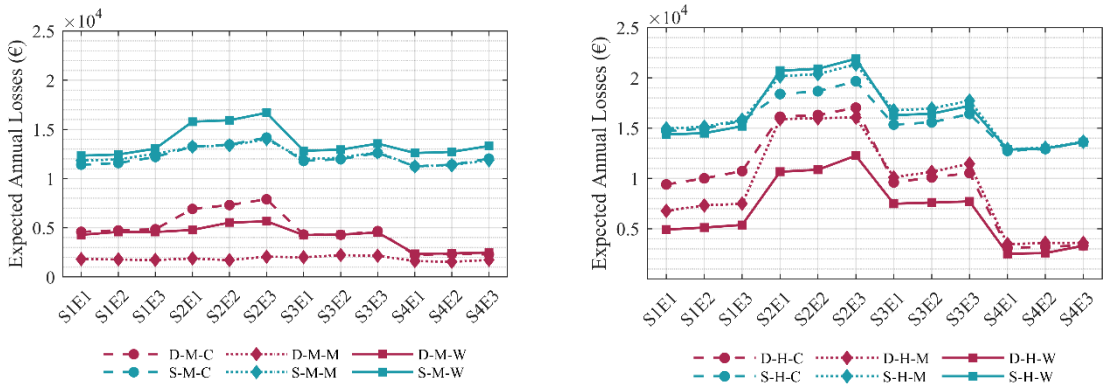

(a) (b)

Figure 9. EAL values obtained employing the detailed and simplified methodologies for: (a) medium and (b) high hazard sites.

3.5. Post-Intervention Energy Assessment

The energy performance of the as-built and energy-retrofitted buildings was assessed with EDILCLIMA [54]. The information regarding the energy modelling and all the assumptions made are detailed in [11]. The energy performance was assessed through different parameters, including the primary energy performance (PEC), equivalent CO_2 emissions (Eq. CO_2), annual energy costs (AEC), and Italian energy class rating. The results obtained for the as-built and energy-retrofitted building are summarized in Table 11. As anticipated, all retrofit schemes resulted in improvements to the energy performance of the structure. Among them, E_3 demonstrated the highest performance, followed by E_2 and E_1 in a progressively incremental manner. This observation underlines the challenge of identifying the optimal energy intervention level solely through direct comparison of these variables, highlighting the necessity for additional criteria in the evaluation process. Indeed, the first level of retrofit (E_1) results in a 28% reduction in the annual PEC, while E_2 and E_3 retrofit

 doi:10.20944/preprints202404.0748.v1

schemes exhibit reductions of about 50% and 80% respectively. Similar trends are observed for Eq. CO_2 and AEC.

Table 9. Energy performance assessment results.

Alt.	PEC (kWh/m²)	Eq. CO_2 (kgCO_2e)	AEC (€)	Energy Class
E_0	309	76,651	12,718	E
E_1	221.76 (*-28%*)	52,476 (*-32%*)	8,765 (*-31%*)	D
E_2	166.63 (*-46%*)	40,716 (*-47%*)	7,121 (*-44%*)	C
E_3	64.92 (*-79%*)	14,982 (*-80%*)	3,109 (*-76%*)	A2

Note: In brackets the reduction (%) of PEC, Eq. CO_2 and AEC, for each energy-retrofitting intervention, with respect to the as-built condition.

4. Discussion

4.1. Decision Variable Assemblance

In this section, all the DVs for each combined retrofitted scheme and each site are quantified. The methods that were used to quantify the DVs, together with the assumptions made and the weight vectors assumed, are detailed in [11].

The installation cost (C_1) and duration of works (C_5) of the combined retrofit alternatives are summarized in Table 5. The expected annual cost (C_2) encompasses the EAL, the AEC and the maintenance cost of the retrofit components. The EAL and the AEC were determined from the seismic and energy performance analyses carried out in the previous sections. The cost of the structural maintenance over the lifetime of the structure (75 years) was obtained considering the interventions outlined by Caterino et al. [9] and scaling them based on the quantity of materials used. The expected LCEI (C_3) includes the installation EI of the retrofit alternative, the EAEI of the retrofitted structure and the total maintenance EI of the alternative over the expected service life. The EIs associated with the installation and maintenance of the retrofit alternatives were estimated using the EEIOLCA procedure (described in [43]), while the EAEI values were obtained from the loss assessment (Section 3.4.2). The values of the annual probability of failure (C_4) were determined in Section 3.4.1. The remaining DVs – architectural impact (C_6), need for specialized labour/design knowledge (C_7), and required interventions at the foundations (C_8) – were set according to [11].

The DVs directly linked to the seismic performance of the structure, namely C_2, C_3 and C_4, are the only DVs whose quantifications depend on the employed methodology. The final values for such DVs are detailed in Table 12 and Table 13 for the medium and high hazard sites, respectively. The remaining DVs (C_1, C_6, C_7 and C_8), which are independent from the employed approach, are outlined in Table 14.

Table 10. DVs C_2, C_3 and C_4 for the medium hazard sites.

	Detailed									Simplified								
	C			M			W			C			M			W		
Alt	C_2	C_3	C_4	C_2	C_3	C_4	C_2	C_3	C_4	C_2	C_3	C_4	C_2	C_3	C_4	C_2	C_3	C_4
S_1E_1	9.5	25.4	1.22	10.4	43.2	0.36	13.5	52.7	1.30	15.3	29.2	1.19	18.0	48.2	0.25	18.9	56.3	1.38
S_1E_2	9.5	21.6	1.28	9.6	35.3	0.33	12.5	42.5	1.31	15.2	25.3	1.19	17.4	40.4	0.25	18.0	46.1	1.38
S_1E_3	8.8	14.8	1.20	7.4	18.0	0.31	9.9	21.4	1.28	14.8	18.7	1.19	15.6	23.4	0.25	15.7	25.2	1.38
S_2E_1	9.0	23.5	1.14	9.5	41.1	0.26	14.2	51.8	1.95	16.8	28.9	1.33	17.1	46.2	0.35	18.8	54.8	1.49
S_2E_2	9.3	19.9	1.40	8.7	33.2	0.19	13.5	41.7	2.08	16.8	25.0	1.33	16.4	38.4	0.35	17.9	44.6	1.49

Preprints.org (www.preprints.org) | NOT PEER-REVIEWED | Posted: 11 April 2024 doi:10.20944/preprints202404.0748.v1

S_2E_3	8.6	13.1	1.39	6.7	16.1	0.30	11.1	20.8	2.18	16.5	18.5	1.33	14.6	21.4	0.35	15.6	23.8	1.49
S_3E_1	8.7	22.4	0.93	9.7	40.3	0.28	12.5	49.6	0.96	15.3	26.9	1.37	17.2	45.4	0.32	18.2	53.4	1.56
S_3E_2	8.6	18.4	0.95	9.2	32.6	0.37	11.4	39.3	0.92	15.2	23.0	1.37	16.6	37.6	0.32	17.2	43.3	1.56
S_3E_3	8.0	11.7	0.96	6.9	15.3	0.32	8.9	18.3	0.98	14.5	16.5	1.37	14.8	20.6	0.32	14.9	22.4	1.56
S_4E_1	8.6	21.8	0.53	10.7	40.5	0.30	12.3	49.0	0.46	16.2	26.8	0.11	17.9	45.2	0.00	18.8	53.8	0.17
S_4E_2	8.5	17.9	0.54	9.9	32.6	0.27	11.3	38.7	0.49	16.1	22.9	0.11	17.3	37.4	0.00	17.9	43.1	0.17
S_4E_3	7.8	11.1	0.54	7.9	15.4	0.31	8.5	17.5	0.44	15.8	16.4	0.11	15.4	20.4	0.00	15.6	22.2	0.17

*Note: The units of C_2 and C_3 are respectively: € and $kgCO_2e$. C_4 is unitless ($x10^{-3}$).

Table 11. DVs C_2, C_3 and C_4 for the high hazard sites.

	Detailed									Simplified								
	C			M			W			C			M			W		
Alt	C_2	C_3	C_4	C_2	C_3	C_4	C_2	C_3	C_4	C_2	C_3	C_4	C_2	C_3	C_4	C_2	C_3	C_4
S_1E_1	12.9	28.4	1.01	16.2	40.4	1.68	18.8	47.5	2.67	19.7	33.0	0.91	22.7	52.3	1.42	23.7	60.3	1.20
S_1E_2	12.9	24.5	1.08	14.3	23.4	1.87	16.5	26.6	2.90	19.6	29.1	0.91	22.1	44.5	1.42	22.8	50.2	1.20
S_1E_3	12.3	17.9	1.12	13.4	42.7	1.81	16.9	52.5	2.94	19.3	22.6	0.91	20.4	27.5	1.42	20.6	29.4	1.20
S_2E_1	13.1	25.0	2.86	18.8	38.7	4.55	19.7	44.6	4.58	20.3	30.1	1.36	22.5	48.9	2.05	22.4	56.2	1.81
S_2E_2	13.1	21.2	2.93	16.6	21.5	4.70	17.3	23.5	4.73	20.3	26.3	1.36	22.1	41.5	2.05	21.5	46.1	1.81
S_2E_3	13.3	15.1	3.30	22.3	47.2	4.37	24.2	55.9	4.64	20.2	19.9	1.36	20.5	24.3	2.05	19.5	25.1	1.81
S_3E_1	13.6	23.9	1.66	17.4	36.3	2.46	17.8	41.7	2.05	19.8	28.5	0.65	22.8	47.1	1.04	23.0	55.2	0.85
S_3E_2	13.5	20.0	1.67	15.5	19.3	2.66	15.4	20.8	2.38	19.8	24.6	0.65	22.2	40.0	1.04	22.1	45.5	0.85
S_3E_3	12.8	13.3	1.62	22.8	45.6	2.74	23.3	53.3	2.27	19.6	18.2	0.65	20.6	23.1	1.04	19.9	24.3	0.85
S_4E_1	13.7	22.6	0.40	16.3	34.2	0.70	16.9	39.8	0.52	21.2	27.6	0.02	23.8	46.6	0.00	24.8	54.7	0.03
S_4E_2	13.6	18.7	0.40	14.2	19.2	0.74	14.8	20.8	0.57	21.1	23.7	0.02	23.2	38.9	0.00	23.9	44.6	0.03
S_4E_3	13.4	14.4	0.59	2.61	1.58	0.68	2.41	1.48	0.54	20.7	19.4	0.02	21.4	24.0	0.00	21.6	25.9	0.03

*Note: The units of C_2 and C_3 are respectively: € and $kgCO_2e$. C_4 is unitless ($x10^{-3}$).

Table 12. DVs C_6 and C_8 for the medium and high hazard sites.

Alt.	C_6 (-)	C_7 (-)	C_8 (-)					
			Medium hazard			High hazard		
			M-C	M-M	M-W	H-C	H-M	H-W
S_1E_1	0.023	0.084	5.9	6.2	7.0	6.1	5.7	5.7
S_1E_2	0.023	0.084	5.9	6.2	7.0	6.1	5.7	5.7
S_1E_3	0.023	0.084	5.9	6.2	7.0	6.1	5.7	5.7

 doi:10.20944/preprints202404.0748.v1

S_2E_1	0.056	0.013	10.9	11.3	12.5	16.5	16.5	16.5
S_2E_2	0.056	0.013	10.9	11.3	12.5	16.5	16.5	16.5
S_2E_3	0.056	0.013	10.9	11.3	12.5	16.5	16.5	16.5
S_3E_1	0.093	0.084	12.8	13.4	13.0	16.6	16.6	16.6
S_3E_2	0.093	0.084	12.8	13.4	13.0	16.6	16.6	16.6
S_3E_3	0.093	0.084	12.8	13.4	13.0	16.6	16.6	16.6
S_4E_1	0.162	0.151	3.3	3.5	3.9	5.1	4.8	4.8
S_4E_2	0.162	0.151	3.3	3.5	3.9	5.1	4.8	4.8
S_4E_3	0.162	0.151	3.3	3.5	3.9	5.1	4.8	4.8

4.2. Ranking of the Retrofit Alternatives

The DVs quantified in the previous sections were then used as input for the MCDM framework. The position of each alternative in the ranking is given by the relative closeness, which is a measure used to assess the proximity of each alternative to an ideal solution or reference point and is often expressed as a value between 0 and 1. A relative closeness value of 1 indicates that the alternative is the most desirable or closest to the ideal solution, while a value closer to 0 suggests lower desirability or greater distance from the ideal solution. This measure allows decision-makers to quantitatively evaluate and rank different alternatives, facilitating the selection of the most favourable option based on the specified criteria and their respective importance weights. According to the number of retrofit alternatives investigated herein, those occupying positions 1 and 12 are regarded as the most and least preferred options, respectively. The preferential rankings obtained for each approach and hazard level are presented in Table 14.

Table 13. Classification ranking of the retrofit alternatives as a function of hazard level, employed approach and climate site.

Rank	Medium Hazard						High Hazard					
	Detailed			Simplified			Detailed			Simplified		
	C	M	W	C	M	W	C	M	W	C	M	W
1	S_3E_3	S_2E_3	S_3E_2	S_4E_1	S_4E_1	S_4E_1	S_3E_3	S_4E_3	S_4E_2	S_4E_2	S_4E_2	S_4E_2
2	S_4E_3	S_2E_2	S_4E_1	S_4E_2	S_4E_2	S_4E_2	S_4E_3	S_4E_2	S_4E_1	S_3E_3	S_4E_3	S_4E_1
3	S_4E_2	S_3E_3	S_2E_1	S_4E_3	S_4E_3	S_2E_1	S_4E_2	S_3E_3	S_4E_3	S_4E_3	S_4E_1	S_4E_3
4	S_3E_2	S_2E_1	S_3E_1	S_2E_2	S_2E_2	S_2E_2	S_3E_2	S_4E_1	S_3E_2	S_3E_2	S_3E_3	S_3E_2
5	S_4E_1	S_3E_2	S_4E_2	S_2E_3	S_2E_1	S_4E_3	S_3E_1	S_3E_2	S_3E_3	S_4E_1	S_3E_2	S_3E_1
6	S_3E_1	S_4E_3	S_3E_3	S_2E_1	S_2E_3	S_3E_1	S_4E_1	S_2E_3	S_3E_1	S_3E_1	S_3E_1	S_3E_3
7	S_2E_3	S_3E_1	S_2E_2	S_3E_2	S_3E_2	S_3E_2	S_2E_3	S_3E_1	S_2E_2	S_2E_3	S_2E_3	S_2E_2
8	S_2E_2	S_4E_1	S_2E_3	S_3E_1	S_3E_3	S_2E_3	S_2E_2	S_2E_2	S_2E_1	S_2E_2	S_2E_2	S_2E_1
9	S_2E_1	S_4E_2	S_4E_3	S_3E_3	S_3E_1	S_3E_3	S_2E_1	S_2E_1	S_2E_3	S_2E_1	S_2E_1	S_2E_3
10	S_1E_3	S_1E_3	S_1E_3	S_1E_3	S_1E_3	S_1E_1	S_1E_3	S_1E_3	S_1E_2	S_1E_3	S_1E_3	S_1E_2
11	S_1E_2	S_1E_2	S_1E_1	S_1E_2	S_1E_2	S_1E_2	S_1E_1	S_1E_1	S_1E_1	S_1E_2	S_1E_2	S_1E_1
12	S_1E_1	S_1E_1	S_1E_2	S_1E_1	S_1E_1	S_1E_3	S_1E_2	S_1E_2	S_1E_3	S_1E_1	S_1E_1	S_1E_3

It is firstly seen that the classification ranking of the retrofit alternatives changes with the seismic hazard level. For the high hazard sites, a clear trend is observed: the rankings of the alternatives tend to be grouped by the structural retrofit scheme option, with S_4 being the most preferred option followed by S_3, S_2 and, lastly, S_1. This trend indicates that the seismic retrofit scheme has a more significant effect on the overall ranking of an alternative than the energy retrofit scheme, as was also highlighted in [11]. Nevertheless, inside each structural retrofit group, the energy retrofitting tends to be ranked according to the energy needs of the site, i.e. the preferential position shifts as a function of the climate conditions, favouring E_3 under cold climate and E_1 under warm climate. In contrast,

 doi:10.20944/preprints202404.0748.v1

for medium seismic hazard sites, the ranking is equally affected by both types of retrofit interventions. S_3 and S_4 are generally preferred as the structural retrofit, except for the moderate climate site. In fact, due to similar performance values of APF, EAL, and EAEI, the MCDM framework struggles to discern distinct benefits among alternatives.

Comparing the results obtained through both detailed and simplified approaches, for the medium hazard sites, the simplified one aligns rankings based on the structural retrofit scheme, with S_4 being the favoured option, followed by S_2, S_3, and S_1. Overall, the main difference between the detailed and simplified approaches is the ranking positions of alternatives S_2 and S_3, which is in line with the trends highlighted by the collapse assessment results. Considering the high hazard sites, even though the exact DV values estimated by the different approaches can be relatively different, at times, the final ranking of the different retrofit alternatives is practically the same, with only a few exceptions observed. For both detailed and simplified approaches, regardless of the hazard level, alternative S_1 is consistently ranked as the least preferred alternative, mainly due to its high installation costs, which are two to six times higher than the other alternatives. This happens because S_1 requires, to control the structural drifts, many CFRP bars, which are costly and labour-intensive to install.

Since the ranking is controlled by the relative closeness value obtained for each retrofit alternative, the way it changes with the level of detail of the adopted approach and the hazard level is also investigated. This can also enable more comprehensive conclusions on the reliability of the simplified methodology, regardless of some slight changes noted in the classification rankings of the retrofit alternatives. Accordingly, Figure 10 shows the relative closeness values of each alternative. In these subplots, the retrofitting alternatives along the X axis are sorted according to the detailed approach ranking.

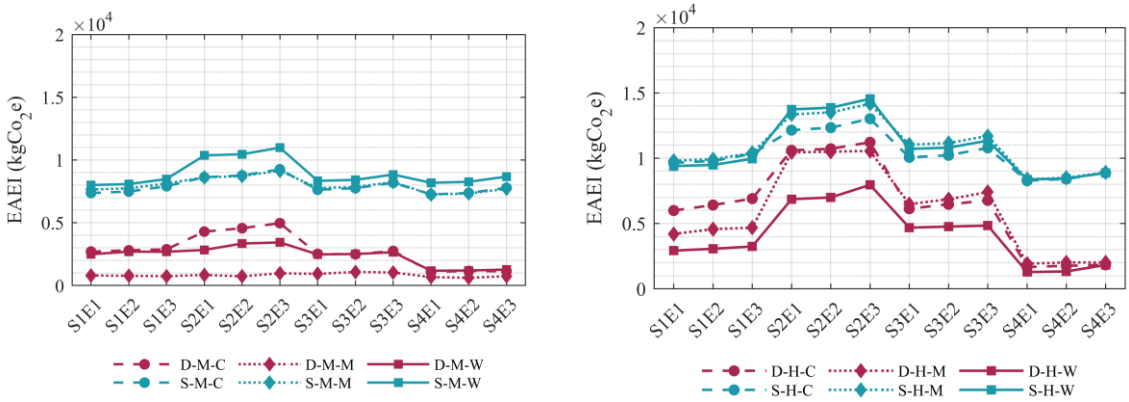

Figure 10. EAEI values obtained employing the detailed and simplified methodologies for: (a) medium and (b) high hazard sites.

Regarding the medium hazard sites, a general mismatch between the different approaches is observed, regardless of climate conditions. A closer scrutinization of these results shows a suitable alignment between the alternatives with S_1 and S_4 as structural retrofit for the cold and warm climate sites, as previously pointed out. Considering the high hazard sites, all the alternatives demonstrate a strong alignment across all sites, with a slight variation in the relative closeness values between the detailed and simplified approaches being observed for S4 in moderate and warm climates. However, this discrepancy does not impact the overall classification.

According to the MCDM framework, the solution ranked first is considered the optimal solution. However, given the closely similar relative closeness values among certain alternatives, a group of most preferable alternatives may be identified, instead of solely focusing on the top-ranked solution. To do so, the 25th and 75th percentiles of the relative closeness values were quantified for both detailed and simplified approaches, as shown in Figure 10. In this way, three groups of alternatives are

Preprints.org (www.preprints.org) | NOT PEER-REVIEWED | Posted: 11 April 2024 doi:10.20944/preprints202404.0748.v1

obtained, allowing to identify the less (below the 25th percentile), relatively (between the 25th and 75th percentile) and most (above the 75th percentile) preferable alternatives.

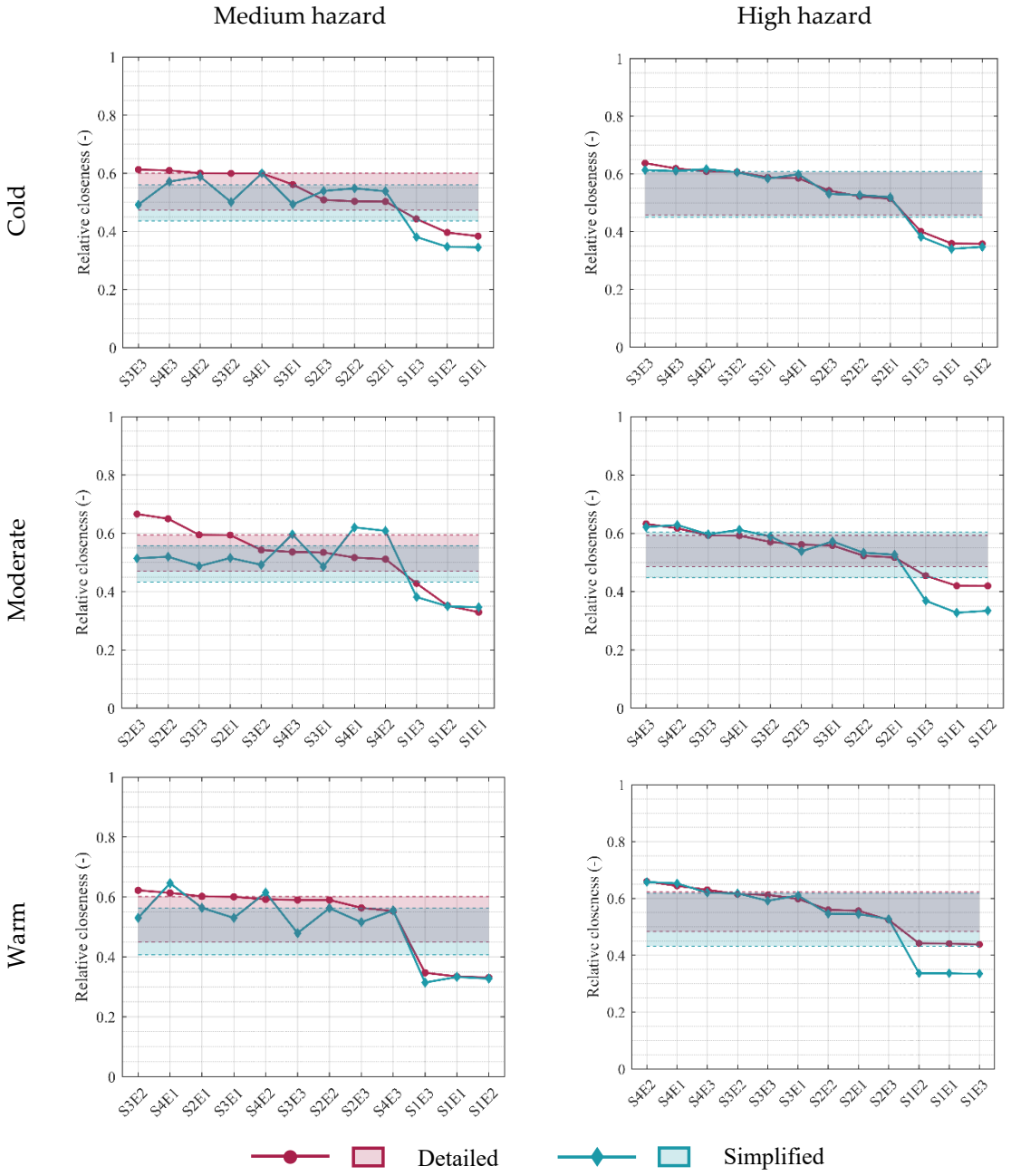

Figure 11. Relative closeness obtained through the detailed and simplified approaches, for different seismic hazard and climate levels.

Table 14 provides the less (red), relatively (yellow) and most (green) preferable alternatives, as a function of the hazard level and the employed approach.

 doi:10.20944/preprints202404.0748.v1

Table 14. Less, medium, and most preferable alternatives, as a function of the location and employed methodology.

Medium Hazard						High Hazard					
Detailed			Simplified			Detailed			Simplified		
C	M	W	C	M	W	C	M	W	C	M	W
S_1E_1	S_1E_1	S_1E_1	S_1E_1	S_1E_1	S_1E_1	S_1E_1	S_1E_1	S_1E_1	S_1E_1	S_1E_1	S_1E_1
S_1E_2	S_1E_2	S_1E_2	S_1E_2	S_1E_2	S_1E_2	S_1E_2	S_1E_2	S_1E_2	S_1E_2	S_1E_2	S_1E_2
S_1E_3	S_1E_3	S_1E_3	S_1E_3	S_1E_3	S_1E_3	S_1E_3	S_1E_3	S_1E_3	S_1E_3	S_1E_3	S_1E_3
S_2E_1	S_2E_1	S_2E_1	S_2E_1	S_2E_1	S_2E_1	S_2E_1	S_2E_1	S_2E_1	S_2E_1	S_2E_1	S_2E_1
S_2E_2	S_2E_2	S_2E_2	S_2E_2	S_2E_2	S_2E_2	S_2E_2	S_2E_2	S_2E_2	S_2E_2	S_2E_2	S_2E_2
S_2E_3	S_2E_3	S_2E_3	S_2E_3	S_2E_3	S_2E_3	S_2E_3	S_2E_3	S_2E_3	S_2E_3	S_2E_3	S_2E_3
S_3E_1	S_3E_1	S_3E_1	S_3E_1	S_3E_1	S_3E_1	S_3E_1	S_3E_1	S_3E_1	S_3E_1	S_3E_1	S_3E_1
S_3E_2	S_3E_2	S_3E_2	S_3E_2	S_3E_2	S_3E_2	S_3E_2	S_3E_2	S_3E_2	S_3E_2	S_3E_2	S_3E_2
S_3E_3	S_3E_3	S_3E_3	S_3E_3	S_3E_3	S_3E_3	S_3E_3	S_3E_3	S_3E_3	S_3E_3	S_3E_3	S_3E_3
S_4E_1	S_4E_1	S_4E_1	S_4E_1	S_4E_1	S_4E_1	S_4E_1	S_4E_1	S_4E_1	S_4E_1	S_4E_1	S_4E_1
S_4E_2	S_4E_2	S_4E_2	S_4E_2	S_4E_2	S_4E_2	S_4E_2	S_4E_2	S_4E_2	S_4E_2	S_4E_2	S_4E_2
S_4E_3	S_4E_3	S_4E_3	S_4E_3	S_4E_3	S_4E_3	S_4E_3	S_4E_3	S_4E_3	S_4E_3	S_4E_3	S_4E_3

The results from Table 14 are aligned with the previous remarks. The optimal group of alternatives varies depending on the climate levels. While cold climate sites lead to a preference for the most demanding energy retrofitting and the structural retrofit with the best structural performance (in accordance with Section 3.4), warm climate sites show only a preference for the structural retrofit with the best performance. Regardless of the employed methodology, the solutions with S_1 as the structural retrofit are always the least preferred options. The shaded area between the 25th and 75th ranking percentiles from each approach (Figure 10) supports the interpretation of the differences between the application of both approaches. While minimal variations are noted in high hazard locations among the alternatives in each preference group, greater disparities are evident in medium hazard locations, mostly for the moderate climate, where the results obtained with the simplified approach are different from the ones obtained with the detailed counterpart. This is likely due the difference in the hazard curves, as observed in Figure 3, which shows how the M-M hazard curve is slightly different from the other medium-hazard locations.

5. Conclusions

This study assessed the influence of diverse seismic hazard and climate conditions on the preferential ranking of combined energy and seismic retrofitting interventions, through the employment of a multi-criteria decision-making (MCDM) framework. Additionally, the accuracy of employing a simplified approach in the estimation of decision variables related to the seismic performance of a building within the MCDM framework, namely the expected annual losses (EAL), annual probability of failure (APF) and expected annual environmental impact (EAEI), was also assessed.

To this end, a case-study school building was selected, and four seismic retrofitting solutions, combined with three energy-based interventions, were identified. The case-study building was assumed to be in six different sites in Italy, characterised by two levels of seismic hazard (moderate (M) and high (H)) and with different climatic conditions, namely cold (C), moderate (M) and warm (W). The performance of the building, in its as-built and retrofitted conditions, was then analysed considering the simplified approach and compared with a more detailed one. Finally, an MCDM framework was employed to obtain the overall ranking of the different alternatives and identify the optimal combination of retrofitting schemes, again using both detailed and simplified approaches.

 doi:10.20944/preprints202404.0748.v1

The preliminary assessment of the structural retrofit models resulted in an effectiveness ranking of the retrofit alternatives as $S_4 > S_1 > S_3 > S_2$ and $S_1 > S_4 > S_3 > S_2$ for the medium and high hazard sites, respectively, for the Life Safety Limit State. Regarding the APF values, notable differences were obtained: while the approaches yielded similar results for medium hazard levels, for the high hazard level, the simplified approach produces lower APF values than the detailed one in high hazard sites, which needs to be considered as trade-off for computational efficiency. Regarding the EAL and EAEI, the simplified approach tends to overestimate EAL with respect to the detailed one. Such overestimation can be attributed to the simplified nature of the Sismabonus procedure, needed to incorporate it into the current Italian seismic risk guidelines in order to enhance its usability by practitioners. Nevertheless, the order of magnitude is kept the same between the different methodologies.

When employing the MCDM framework to obtain the overall ranking of the different alternatives and identify the optimal combination of retrofitting schemes combined with the different detailed and simplified approaches, similar relative closeness values among several alternatives pointed towards the identification of a group of preferable alternatives, instead of the most preferable one. By quantifying the 25th and 75th percentiles of the relative closeness values for both detailed and simplified approaches, three distinct groups of alternatives were identified as less, relatively and most preferable. This approach facilitates the comparison between alternatives with similar relative closeness values, enabling the selection of more than one optimal retrofit alternative in engineering practice.

Globally, the results showed distinct classifications for medium and high seismic hazard sites. For high hazard ones, the influence of the seismic hazard is highly present since rankings tend to be grouped by structural retrofit scheme, and, in most cases, the most severe energy retrofit alternative was generally preferred over the other alternatives. In medium seismic hazard sites, rankings are equally affected by both types of retrofit intervention. For both levels of hazard, S_1 is consistently the least preferable structural retrofit alternative. Even though its seismic performance is relatively better than alternatives S_2 and S_3, its high cost tends to penalize it on the MCDM framework. Comparing both approaches, results show that in high hazard areas, rankings stay consistent, while, in medium hazard sites, detailed and simplified approaches yield different results. In the detailed one, both energy and seismic retrofit play crucial roles, leading to varied rankings, where the simplified method aligns rankings based on the structural retrofit scheme. Despite similar performance values (APF, EAL, and EAEI), the MCDM struggles to point clear preferable alternatives. Nevertheless, the results obtained through the simplified approach are promising, given that the differences observed in the optimal combination ranking, compared to the detailed counterpart, are mainly justified by the relative distance between different alternatives that affect the mathematical process of the MCDM procedure. In fact, although further investigations will support more general conclusions on the reliability of the simplified, practice-oriented approach, from an overall perspective, the employment of the detailed and simplified approaches led to similar results in the obtained ranking, showing the benefits of employing tools that require less time and computational demand.

Author Contributions: R.C: methodology, software, validation, writing—original draft preparation; G.M: supervision, conceptualization, writing—review and editing; R.M: supervision, conceptualization, writing—review and editing; R.B: supervision, conceptualization, writing—review and editing. All authors have read and agreed to the published version of the manuscript.

Funding: This research has been funded by the Italian Civil Protection Department within the framework of the projects "ReLUIS 2022-2024", and financially supported by national Portuguese funds through the FCT/MCTES (PIDDAC), under the project 2022.08138.PTDC.

Conflicts of Interest: The authors declare no conflict of interest.

 doi:10.20944/preprints202404.0748.v1

References

1. European Comission Communication from the Commission to the European Parliament, the Council, the European Economic and Social Committee and the Committee ofthe Regions. The European Green Deal; Brussels, Belgium, 2020;
2. Ministero dell'Ambiente e della Sicurezza Energetica Piano Nazionale Integrato per l'Energia e per il Clima. **2023**.
3. Pohoryles, D.; Bournas, D.; Da Porto, F.; Santarsiero, G.; Triantafillou, G.; Oliveira, D.; Jelle, B. *Technologies for the combined seismic and energy upgrading of existing buildings*; EUR 31012.; Publications Office of the European Union: Luxembourg, 2022; ISBN 978-92-76-49257-3.
4. Gkatzogias, K.; Tsionis, G. Prioritising EU regions for building renovation: seismic risk, energy efficiency; 2022; ISBN 9789276550235.
5. Gkatzogias, K.; Pohoryles, D.A.; Romano, E.; Bournas, D.A. *Integrated seismic and energy renovation of buildings*; 2023;
6. Pohoryles, D.A.; Bournas, D.A.; Da Porto, F.; Santarsiero, G.; Triantafillou, T. *Overview of combined seismic and energy upgrading technologies for existing buildings*; Luxembourg, 2022;
7. Mucedero, G.; Couto, R.; Monteiro, R. Seismic and energy performance upgrading of existing buildings in Italy : seismicity vs . climatic conditions. 2.
8. Asadi, E.; Salman, A.M.; Li, Y. Multi-criteria decision-making for seismic resilience and sustainability assessment of diagrid buildings. *Eng. Struct.* **2019**, *191*, 229–246, doi:10.1016/j.engstruct.2019.04.049.
9. Caterino, N.; Iervolino, I.; Manfredi, G.; Cosenza, E. Multi-Criteria Decision Making for Seismic Retrofitting of RC Structures. *J. Earthq. Eng.* **2008**, *12*, 555–583, doi:10.1080/13632460701572872.
10. Requena-García-Cruz, M.V.; Morales-Esteban, A.; Durand-Neyra, P.; Estêvão, J.M.C. An index-based method for evaluating seismic retrofitting techniques. Application to a reinforced concrete primary school in Huelva. *Earth its Atmos.* **2019**, *14*, doi:10.1371/journal.pone.0215120.
11. Clemett, N.; Carofilis, W.; Gabbianelli, G.; O'Reilly, G.J.; Monteiro, R. Optimal Combined Seismic and Energy Efficiency Retrofitting for Existing Buildings in Italy. *J. Struct. Eng.* **2023**, *149*, 1–16, doi:10.1061/(asce)st.1943-541x.0003500.
12. Caruso, M.; Pinho, R.; Bianchi, F.; Cavalieri, F.; Lemmo, M.T. Integrated economic and environmental building classification and optimal seismic vulnerability/energy efficiency retrofitting; Springer Netherlands, 2021; Vol. 19; ISBN 0123456789.
13. Saler, E.; Gattesco, N.; da Porto, F. A new combined approach to prioritise seismic retrofit interventions on stocks of r.c. school buildings. *Int. J. Disaster Risk Reduct.* **2023**, *93*, 103767, doi:10.1016/j.ijdrr.2023.103767.
14. Couto, R.; Mucedero, G.; Bento, R.; Monteiro, R. ON THE INFLUENCE OF CLIMATE AND SEISMIC HAZARD CONDITIONS IN THE IDENTIFICATION OF OPTIMAL RETROFITTING STRATEGIES FOR RC BUILDINGS. In Proceedings of the COMPDYN Proceedings; 2023; pp. 2070–2084.
15. Caruso, M.; Couto, R.; Pinho, R.; Monteiro, R. Decision-making approaches for optimal seismic/energy integrated retrofitting of existing buildings. *Front. Built Environ.* **2023**, *9*, 1–12, doi:10.3389/fbuil.2023.1176515.
16. Mucedero, G.; Couto, R.; Clemett, N.; Monteiro, R. Implications of masonry infill – related uncertainty on the optimal seismic retrofitting of existing buildings. *14th Int. Conf. Appl. Stat. Probab. Civ. Eng.* **2023**, 1–8.
17. Carofilis, W.; Clemett, N.; Gabbianelli, G.; O'Reilly, G.; Monteiro, R. Influence of Parameter Uncertainty in Multi-Criteria Decision-Making When Identifying Optimal Retrofitting Strategies for RC Buildings. *J. Earthq. Eng.* **2022**, doi:10.1080/13632469.2022.2087794.
18. Vamvatsikos, D.; Cornell, C.A. Direct Estimation of Seismic Demand and Capacity of Multidegree-of-Freedom Systems through Incremental Dynamic Analysis of Single Degree of Freedom Approximation. *J. Struct. Eng.* **2005**, *131*, 589–599, doi:10.1061/(ASCE)0733-9445(2005)131:4(589).
19. Baltzopoulos, G.; Baraschino, R.; Iervolino, I.; Vamvatsikos, D. SPO2FRAG: software for seismic fragility assessment based on static pushover. *Bull. Earthq. Eng.* **2017**, *15*, 4399–4425, doi:10.1007/s10518-017-0145-3.
20. Dolšek, M.; Fajfar, P. IN2 - A Simple Alternative for IDA. *13th World Conf. Earthq. Eng.* **2004**.
21. FEMA P58-1 Seismic Performance Assessment of Buildings: Volume 1 - Methodology. **2018**, *1*, 344, doi:10.4231/D3ZW18S8N.
22. Ramirez, C.M.; Miranda, E. *Building-specific loss estimation methods & tools for simplified performance-based. Report No. 171*; , Blume Center Report. Edited by T. J. A. B. E. E. Center. Stanford, CA., 2009;
23. Mucedero, G.; Perrone, D.; Monteiro, R. Generalised Storey Loss Functions for Seismic Loss Assessment of Italian Residential Buildings. *J. Earthq. Eng.* **2023**, 1–24, doi:10.1080/13632469.2023.2218491.
24. Perrone, G.; Cardone, D.; O'Reilly, G.J.; Sullivan, T.J. Developing a Direct Approach for Estimating Expected Annual Losses of Italian Buildings. *J. Earthq. Eng.* **2022**, *26*, 1–32, doi:10.1080/13632469.2019.1657988.
25. Nettis, A.; Gentile, R.; Raffaele, D.; Uva, G.; Galasso, C. Cloud Capacity Spectrum Method: Accounting for record-to-record variability in fragility analysis using nonlinear static procedures. *Soil Dyn. Earthq. Eng.* **2021**, *150*, 106829, doi:10.1016/j.soildyn.2021.106829.

26. Cosenza, E.; Del Vecchio, C.; Di Ludovico, M.; Dolce, M.; Moroni, C.; Prota, A.; Renzi, E. *The Italian guidelines for seismic risk classification of constructions: technical principles and validation*; Springer Netherlands, 2018; Vol. 16; ISBN 0123456789.
27. FEMA P-58-3: Seismic Performance Assessment of Buildings: Volume 3—Performance Assessment Calculation Tool (PACT). *Washington, DC FEMA.* **2012**.
28. Applied Technology Council (ATC) ATC 40 - Seismic Evaluation and Retrofit of Concrete Buildings. **1996**.
29. Jalayer, F.; Ebrahimian, H.; Miano, A.; Manfredi, G.; Sezen, H. Analytical fragility assessment using unscaled ground motion records. *Earthq. Eng. Struct. Dyn.* **2017**, *46*, 2639–2663, doi:10.1002/eqe.2922.
30. Peres, R.; Couto, R.; Sousa, I.; Castro, J..; Bento, R. Modelling and evaluation of brittle shear effects on the seismic performance and loss assessment of RC buildings. *Eng. Struct.* **2023**.
31. O'Reilly, G.J.; Perrone, D.; Fox, M.; Monteiro, R.; Filiatrault, A. Seismic assessment and loss estimation of existing school buildings in Italy. *Eng. Struct.* **2018**, *168*, 142–162, doi:10.1016/j.engstruct.2018.04.056.
32. Prota, A.; Di Ludovico, M.; Vecchio, C.; Menna, C. Progetto DPC-ReLUIS 2019-2021 WP5: Interventi di rapida esecuzione a basso impatto ed integrati. **2020**, *72*.
33. Mucedero, G.; Perrone, D.; Brunesi, E.; Monteiro, R. Numerical modelling and validation of the response of masonry infilled rc frames using experimental testing results. *Buildings* **2020**, *10*, 1–30, doi:10.3390/buildings10100182.
34. McKenna, F.; Scott, M.H.; Fenves, G.L. Nonlinear Finite-Element Analysis Software Architecture Using Object Composition. *J. Comput. Civ. Eng.* **2010**, *24*, 95–107, doi:10.1061/(ASCE)CP.1943-5487.0000002.
35. Carofilis, W.; Gabbianelli, G.; Monteiro, R. Assessment of Multi-Criteria Evaluation Procedures for Identification of Optimal Seismic Retrofitting Strategies for Existing RC Buildings. *J. Earthq. Eng.* **2021**, *26*, 5539–5572, doi:10.1080/13632469.2021.1878074.
36. MIT NTC 2018: D.M. del Ministero delle Infrastrutture e dei trasporti del 17/01/2018. Aggiorna- mento delle Norme Tecniche per le Costruzioni (in Italian). **2018**.
37. Fajfar, P. A Nonlinear Analysis Method for Performance-Based Seismic Design. *Earthq. Spectra* **2000**, *16*, 573–592, doi:10.1193/1.1586128.
38. O'Reilly, G.J.; Sullivan, T.J. Modeling Techniques for the Seismic Assessment of the Existing Italian RC Frame Structures. *J. Earthq. Eng.* **2019**, *23*, 1262–1296, doi:10.1080/13632469.2017.1360224.
39. Decreto Ministeriale DM n. 58/2020. Linee Guida per la Classificazione del Rischio Sismico delle Costruzioni.; Rome, Italy, 2020;
40. Calvi, G.M. Choices and criteria for seismic strengthening. *J. Earthq. Eng.* **2013**, *17*, 769–802, doi:10.1080/13632469.2013.781556.
41. Economico, I.M.D.S. Decreto interministeriale 26 Giugno 2015, Applicazione delle metodologie di calcolo delle prestazioni energetiche e definizione delle prescrizioni e dei requisiti minimi degli edifici; Rome: Italian Government, 2015;
42. Carofilis, W.; Perrone, D.; O'Reilly, G.J.; Monteiro, R.; Filiatrault, A. Seismic retrofit of existing school buildings in Italy: Performance evaluation and loss estimation. *Eng. Struct.* **2020**, *225*, 111243, doi:10.1016/j.engstruct.2020.111243.
43. Clemett, N.; Carofilis, W.; O'Reilly, G.J.; Gabbianelli, G.; Monteiro, R. Optimal seismic retrofitting of existing buildings considering environmental impact. *Eng. Struct.* **2022**, *250*, 113391, doi:10.1016/j.engstruct.2021.113391.
44. GEM The OpenQuake-engine User Manual. Global Earthquake Model (GEM) Open- Quake Manual for Engine version 3.7.0. **2019**, 183, doi:10.13117 / GEM.OPENQUAKE.MAN.ENGINE.3.7.0.
45. Ancheta, T.D.; Darragh, R.B.; Stewart, J.P.; Seyhan, E.; Silva, W.J.; Chiou, B.S.-J.; Wooddell, K.E.; Graves, R.W.; Kottke, A.R.; Boore, D.M.; et al. NGA-West2 Database. *Earthq. Spectra* **2014**, *30*, 989–1005, doi:10.1193/070913EQS197M.
46. O'Reilly, G.J.; Sullivan, T.J. Quantification of modelling uncertainty in existing Italian RC frames. *Earthq. Eng. Struct. Dyn.* **2018**, *47*, 1054–1074, doi:10.1002/eqe.3005.
47. Mucedero, G.; Perrone, D.; Monteiro, R. Epistemic uncertainty in poorly detailed existing frames accounting for masonry infill variability and RC shear failure. *Earthq. Eng. Struct. Dyn.* **2022**, *51*, 3755–3778, doi:10.1002/eqe.3748.
48. Mucedero, G.; Perrone, D.; Monteiro, R. Infill Variability and Modelling Uncertainty Implications on the Seismic Loss Assessment of an Existing RC Italian School Building. *Appl. Sci.* **2022**, *12*, doi:10.3390/app122312002.
49. Gencturk, B.; Elnashai, A.S. Development and application of an advanced capacity spectrum method. *Eng. Struct.* **2008**, *30*, 3345–3354, doi:10.1016/j.engstruct.2008.05.008.
50. Chopra, A.K.; Goel, R.K. Evaluation of NSP to Estimate Seismic Deformation: SDF Systems. *J. Struct. Eng.* **2000**, *126*, 482–490, doi:10.1061/(ASCE)0733-9445(2000)126:4(482).
51. FEMA P58-4 Seismic Performance Assessment of Buildings Volume 4 – Methodology for Assessing Environmental Impacts. *Fema P-58-4* **2018**, *4*, 122.

 doi:10.20944/preprints202404.0748.v1

52. Couto, R.; Mucedero, G.; Bento, R.; Monteiro, R. A practice-oriented approach for the seismic and energy performance upgrading of existing buildings. *J. Earthq. Eng.*
53. O'Reilly, G.J.; Nafeh, A.M.B.; Shahnazaryan, D. Simplified tools for the risk assessment and classification of existing buildings. *Procedia Struct. Integr.* **2023**, *44*, 1744–1751, doi:10.1016/j.prostr.2023.01.223.
54. Edilclima EC700 Calcolo Prestazioni Energetiche Degli Edifici—Versione 11. 2022.